J|A|C|S
ARTICLES
Published on Web 02/08/2002

Formation and Characterization of Carbon Monoxide Adducts of Iron "Twin Coronet" Porphyrins. Extremely Low CO Affinity and a Strong Negative Polar Effect on Bound CO

Mikiya Matsu-ura, Fumito Tani,* and Yoshinori Naruta*

Contribution from the Institute for Fundamental Research of Organic Chemistry, Kyushu University, Higashi-ku, Fukuoka 812-8581, Japan

Received August 13, 2001

Abstract: The carbon monoxide (CO) adducts of iron "twin coronet" porphyrins (**TCP**s) are characterized by UV−vis, resonance Raman (RR), IR, and ^{13}C NMR spectroscopies. A superstructured porphyrin, designated as **TCP**, was used as a common framework for the four different types of iron complexes. **TCP** bears two binaphthalene bridges on each side and creates two hydrophobic pockets surrounded by the bulky aromatic rings. In the CO-binding cavities, the hydroxyl groups are oriented toward the center above the heme. The iron complexes investigated are as follows: **TCP** (which is without a covalently linked axial ligand), **TCP**−**PY** (which has a linked pyridine ligand), and **TCP**−**TB** and **TCP**−**TG** (both of which have a linked thiolate ligand). These complexes were synthesized as ferric forms and identified by the various spectroscopic methods. The UV−vis spectra of **TCP**−CO and **TCP**−**PY**−CO exhibit λ_{max} at 432, 546 and 428, 541 nm, respectively. On the other hand, the CO adducts of **TCP**−**TB** and **TCP**−**TG** show typical hyperporphyrin spectra for a thiolate-ligated iron(II) porphyrin-CO complex. In the RR spectra, the ν(Fe−CO) bands were observed at 506, 489 cm^{-1} (**TCP**), 465 cm^{-1} (**TCP**−**PY**), 458, 437 cm^{-1} (**TCP**−**TG**) and 429 cm^{-1} (**TCP**−**TB**). Compared with the reported ν(Fe−CO) frequencies of hemoproteins and their model systems, these observed values are unusually low. Further, abnormally high ν(C−O) bands are observed at 1990 cm^{-1} (**TCP**−CO) and 2008 cm^{-1} (**TCP**−**PY**−CO) in IR spectra. The lower ν(Fe−CO) and the higher ν(C−O) frequencies can be ascribed to the strong negative polar effect caused by the vicinal hydroxyl groups in the cavity. This prediction is further supported by the observation of significant ^{13}C shieldings exhibited by **TCP**−CO ($\delta = 202.6$ ppm) and **TCP**−**PY**−CO ($\delta = 202.3$ ppm), in comparison to hemoproteins and other heme models. The CO affinity of **TCP**−**PY** ($P_{1/2}CO = 0.017$ Torr at 25 °C) is unusually lower than other heme models. The unique behavior of these CO adducts is discussed in context of the **TCP** structures.

Introduction

The binding of small molecules such as carbon monoxide (CO) and dioxygen (O_2) to the active site in hemoproteins has aroused considerable interest during the last few decades. A central question that has led to intense study of biological and model systems is how CO/O_2 discrimination occurs in myoglobin (Mb) and hemoglobin (Hb).[1,2] It had been long assumed that CO/O_2 discrimination is based mainly on distal steric constraints.[3] As a result, most of the model porphyrins had straps or caps containing bulky groups with the aim of sterically impeding CO binding, which intrinsically prefers a linear upright binding conformation.[2,4] More recently, the emphasis has shifted to polar interactions in the binding pocket.[1a,5] That is, a polar environment could favor the highly polarized $Fe^{\delta+}-O-O^{\delta-}$ unit over the apolar Fe−C−O moiety. A limited number of hemoprotein models, which were designed to incorporate polar residues in the binding site, have been reported to date.[2,6,7]

* To whom correspondence should be addressed.

(1) (a) Springer, B. A.; Sligar, S. G.; Olson, J. S.; Phillips, G. N., Jr. *Chem. Rev.* **1994**, *94*, 699. (b) Jameson, G. B.; Ibers, J. A. In *Bioinorganic Chemistry*; Bertini, I., Gray, H. B., Lippard, S. J., Valentine, J. S., Eds.; University Science Books: Mill Valley, CA, 1994; p 167 and references therein.

(2) Momenteau, M.; Reed, C. A. *Chem. Rev.* **1994**, *94*, 659 and references therein.

(3) (a) Collman, J. P.; Brauman, J. I.; Halbert, T. R.; Suslick, K. S. *Proc. Natl. Acad. Sci. U.S.A.* **1976**, *73*, 3333. (b) Stryer, L. *Biochemistry*, 3rd ed.; Freeman: New York, 1988; p 149.

(4) For typical examples, see (a) Peng, S.; Ibers, J. A. *J. Am. Chem. Soc.* **1976**, *98*, 8032. (b) Collman, J. P.; Brauman, J. I.; Collins, T. J.; Iverson, B.; Sessler, J. L. *J. Am. Chem. Soc.* **1981**, *103*, 2450. (c) Collman, J. P.; Brauman, J. I.; Collins, T. J.; Iverson, B.; Lang, G.; Pettman, R. B.; Sessler, J. L.; Walters, M. A. *J. Am. Chem. Soc.* **1983**, *105*, 3038.

(5) (a) Phillips, S. E. V.; Schoenborn, B. P. *Nature* **1981**, *292*, 81. (b) Shaanan, B. *Nature* **1982**, *296*, 683. (c) Traylor, T. G.; Koga, N.; Deardurff, L. A. *J. Am. Chem. Soc.* **1985**, *107*, 6504. (d) Traylor, T. G.; Tsuchiya, S.; Campbell, D.; Mitchell, M.; Stynes, D.; Koga, N. *J. Am. Chem. Soc.* **1985**, *107*, 604. (e) Spiro, T. G.; Kozlowski, P. M. *J. Biol. Inorg. Chem.* **1997**, *2*, 516. (f) Olson, J. S.; Phillips, G. N., Jr. *J. Biol. Inorg. Chem.* **1997**, *2*, 544. (g) Spiro, T. G.; Kozlowski, P. M. *Acc. Chem. Res.* **2001**, *34*, 137.

(6) For typical examples, see (a) Momenteau, M.; Loock, B.; Tetreau, C.; Lavalette, D.; Croisy, A.; Schaeffer, C.; Huel, C.; Lhoste, J.-M. *J. Chem. Soc., Perkin. Trans. 2* **1987**, 249. (b) Wuenschell, G. E.; Tetreau, C.; Lavalette, D.; Reed, C. A. *J. Am. Chem. Soc.* **1992**, *114*, 3346. (c) Chang, C. K.; Liang, Y.; Aviles, G. *J. Am. Chem. Soc.* **1995**, *117*, 4191.

(7) (a) Tani, F.; Nakayama, S.; Ichimura, M.; Nakamura, N.; Naruta, Y. *Chem. Lett.* **1999**, 729. (b) Matsu-ura, M.; Tani, F.; Nakayama, S.; Nakamura, N.; Naruta, Y. *Angew. Chem., Int. Ed.* **2000**, *39*, 1989. (c) Tani, F.; Matsu-ura, M.; Nakayama, S.; Ichimura, M.; Nakamura, N.; Naruta, Y. *J. Am. Chem. Soc.* **2001**, *123*, 1133. (d) Matsu-ura, M.; Tani, F.; Naruta, Y. *Chem. Lett.* **2000**, 814.

10.1021/ja011963g CCC: $22.00

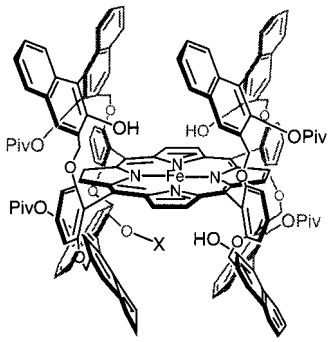

TCP; X = H

TCP-PY; X =

TCP-TB; X =

TCP-TG; X =

Figure 1. Structures of **TCP**, **TCP−PY**, **TCP−TB,** and **TCP−TG**.

CO adducts of globins and iron porphyrin model systems have been employed for investigations of the effects of the ligand-binding environment on the CO/O_2 binding. Many spectroscopic data have been accumulated on CO adducts because of the stability of CO adducts relative to O_2 adducts. The vibrational frequencies of the FeCO unit, readily available from resonance Raman (RR) and infrared (IR) spectroscopy,[8] and the ^{13}C and ^{17}O NMR parameters[9] are sufficiently sensitive to subtle environmental alterations to provide useful indicators of the active site. Using RR and IR spectroscopies, several researchers have noted a negative linear correlation between the ν(Fe−CO) and ν(C−O) frequencies for a variety of heme−CO adducts and have discussed this effect in terms of back-bonding in the FeCO unit.[8a,10−12] Back-donation of Fe^{II} d_π electrons to the CO π^* orbitals increases the Fe−CO bond order while decreasing the C−O bond order. A wide range of ν(Fe−CO) and ν(C−O) values are observed for hemoproteins and their models, but when these values are plotted against each other, most pairs of data fall on a single line, provided that the trans axial ligand is held constant. A good linear correlation between the ^{13}C chemical shift and ν(C−O) frequency has also been noted and explained on the basis of back-bonding changes as modulated by electrostatic interactions of bound CO with the surrounding.[9a,9d] Using these spectroscopic data, the polarity of the binding site has been investigated for various globin mutants and models,[1a,2,9] with the ultimate aim of understanding the mechanism of CO/O_2 discrimination.

To evaluate the polar interaction at the active site, we have synthesized several superstructured porphyrins, **TCP**, **TCP−PY**, **TCP−TB,** and **TCP−TG** (Figure 1), and have examined the vibrational frequencies of the FeCO unit, the ^{13}C chemical shifts, and the binding affinity for CO. On both sides of the porphyrin plane, bulky binaphthyl moieties can form hydrophobic molecular cavities, which are suitable for the binding of small molecules. In the proximal site, pyridine or alkanethiolate groups are covalently fixed to coordinate axially to the central iron and are sterically well sheltered from other oxidative decomposition. In the distal site, two naphtholic hydroxyl groups are oriented toward the center above the heme. In RR spectra, the ν(Fe−CO) and δ(Fe−C−O) modes of **TCP**s−CO adducts were determined, and the proximal factors affecting the strength of Fe−C bond in different axial ligands were investigated. Compared with the reported ν(Fe−CO) and ν(C−O) frequencies of hemoproteins and their models, both the unusually lower ν(Fe−CO) and the unusually higher ν(C−O) frequencies of **TCP**s are notable results. In ^{13}C NMR, significant shielding of the ^{13}C resonance is also observed in our model systems. The CO affinity of **TCP−PY** is extremely low in comparison with other heme models. We, therefore, conclude that the unique physical behaviors observed in RR, IR, ^{13}C NMR, and CO binding affinity are caused by the negative polar interactions of bound CO with the oxygen atom lone pairs of the distal hydroxyl groups.

Results and Discussion

Synthesis and Spectroscopic Characterization of Iron "Twin Coronet" Porphyrins. The"twin coronet" porphyrin (TCP), which bears four binaphthalene bridges on both sides and forms two hydrophobic pockets surrounded by the bulky aromatic rings, is used as a common framework. According to the procedures of the previous report,[7c] the major framework is prepared by condensation of the octahydroxylated TPP **1** and the binaphthyl derivative **2** under basic conditions (Scheme 1). The deprotection and the selective reprotection of the naphthol hydroxyl groups are carried out to afford the free base **5**.

The synthesis of the new complex, **TCP−PY**, which has a pyridine moiety as an axial ligand, is as follows: nicotinic acid is connected to one of the inner hydroxyl groups of **5** by employing EDC (1-(3-(dimethylamino)-propyl)-3-ethylcarbodiimide). The ^1H NMR spectrum of **6** shows fairly complicated splitting patterns: eight mutually coupled doublets for pyrrole β-protons and four singlets for pivaloyl groups. These ^1H NMR features indicate complete loss of the symmetry in **6**, in contrast to the symmetric spectra of **3**−**5** (D_2 symmetry).[13] The chemical shifts of the pyridine moiety, which is strongly shielded by the porphyrin ring current, are significantly shifted to upper field. A singlet for py-H^2, two doublets for py-H^4 and for py-H^6, and a double doublet for py-H^5 are observed (Table 1). The free base porphyrin **6** is converted to the corresponding ferric chloride complex **TCP−PY**−Cl with $Fe(CO)_5$ and I_2. The free base porphyrin **5**, which is without a covalently linked axial ligand in the cavity, is converted to ferric **TCP**−Cl complex by the same method. The synthesis and characterization of thiolate-coordinated heme complexes, **TCP−TB** and **TCP−TG**, have been reported previously.[7c]

(8) (a) *Biological Applications of Raman Spectroscopy*; Spiro, T. G., Ed.; John Wiley: New York, 1988; Vol. 3. (b) Yu, N.-T. *Methods Enzymol.* **1986**, *130*, 350.
(9) (a) Park, K. D.; Guo, K.; Adebodun, F.; Chiu, M. L.; Sligar, S. G.; Oldfield, E. *Biochemistry* **1991**, *30*, 2333. (b) Augspurger, J. D.; Dykstra, C. E.; Oldfield, E. *J. Am. Chem. Soc.* **1991**, *113*, 2447. (c) Oldfield, E.; Guo, K.; Augspurger, J. D.; Dykstra, C. E. *J. Am. Chem. Soc.* **1991**, *113*, 7537. (d) Kalodimos, C. G.; Gerothanassis, I. P.; Pierattelli, R.; Ancian, B. *Inorg. Chem.* **1999**, *38*, 4283.
(10) Li, X. Y.; Spiro, T. G. *J. Am. Chem. Soc.* **1988**, *110*, 6024.
(11) (a) Tsubaki, M.; Ichikawa, Y. *Biochim. Biophys. Acta* **1985**, *827*, 268. (b) Paul, J.; Smith, M. L.; Paul, K.-G. *Biochim. Biophys. Acta* **1985**, *832*, 257. (c) Tsubaki, M.; Hiwatashi, A.; Ichikawa, Y. *Biochemistry* **1986**, *25*, 3563.
(12) Uno, T.; Nishimura, Y.; Tsuboi, M.; Makino, R.; Iizuka, T.; Ishimura, Y. *J. Biol. Chem.* **1987**, *262*, 4549.
(13) For example, ^1H NMR spectrum of **5** shows two singlets for pyrrole β-protons at 8.77 and 8.41 ppm and a singlet for pivaloyl groups at 0.51 ppm.

Scheme 1 [a]

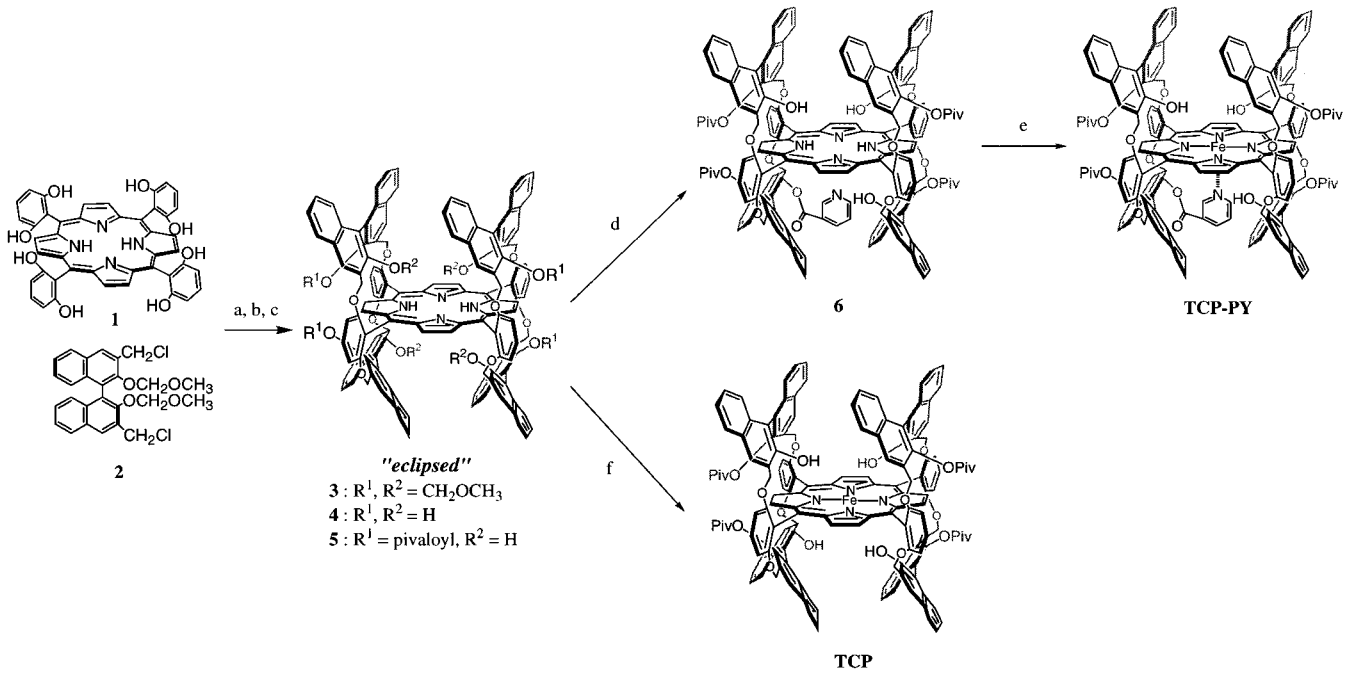

[a] Reagents and conditions: (a) K_2CO_3, THF, NMP, 110 °C, 19%. (b) trimethylsilyl bromide, CH_2Cl_2, −40 °C, 96%. (c) pivaloyl chloride, pyridine, CH_2Cl_2, 97%. (d) nicotinic acid, 1-(3-dimethylamino-propyl)-3-ethylcarbodiimide hydrochloride, 4-dimethylamino-pyridine, CH_2Cl_2, 57%. (e) $Fe(CO)_5$, I_2, toluene, 50 °C, 70%. (f) $Fe(CO)_5$, I_2, toluene, 50 °C, 57%.

Table 1. ^{1}H NMR Data of Methyl Nicotinate and the Pyridine Moiety in **6** and **TCP**−**PY**−CO

compound	py-H^2 (*s*)	$\Delta\delta$[a]	py-H^4 (*d*)	$\Delta\delta$[a]	py-H^5 (*dd*)	$\Delta\delta$[a]	py-H^6 (*d*)	$\Delta\delta$[a]
methyl nicotinate	9.21		8.29 (7.9 Hz)		7.39 (7.9, 4.9 Hz)		8.77 (4.9 Hz)	
6	5.61	−3.6	3.72 (7.8 Hz)	−4.57	4.32 (7.8, 4.9 Hz)	−3.07	6.33 (4.9 Hz)	−2.44
(**TCP**−**PY**)Fe− CO	n.d.[b]		4.58 (7.8 Hz)	−3.71	2.96 (7.8, 5.9 Hz)	−4.43	1.73 (5.9 Hz)	−7.04

[a] $\Delta\delta = \delta$ (**TCP** derivative) − δ (methyl nicotinate). [b] Not determined.

The ESI-MS spectra of **TCP**−**PY**−Cl and **TCP**−Cl exhibit molecular ion peaks at m/z = 2478.9 and 2374.1, respectively. The isotopic patterns are in good agreement with their simulations. Moreover, the observed mass numbers in high-resolution FAB-MS are also in accord with the calculated mass numbers. These data confirm the synthesis of the desired complexes. The ESR spectra of **TCP**−**PY**−Cl and **TCP**-Cl in toluene at 4 K clearly show typical high-spin signals (**TCP**−**PY**−Cl: g = 5.82, 2.00, **TCP**−Cl: g = 5.96, 2.01). In contrast, the thiolate-coordinated heme complexes exhibit rhombic low-spin signals (**TCP**−**TB**: g = 2.334, 2.210, 1.959, **TCP**−**TG**: 2.313, 2.209, 1.966).[7c]

Formation and UV−**Vis Spectra of CO Adducts.** Ferrous **TCP** and **TCP**−**PY** were formed by dithionite reduction. The UV−vis spectrum of ferrous **TCP** in a noncoordinating solvent, such as toluene, exhibits split Soret bands (Table 2) that are characteristic of a four-coordinate ferrous form[14] and a single Soret band is observed in THF, a coordinating solvent. On the other hand, ferrous **TCP**−**PY** has a single Soret band, even in toluene. These results indicate that THF coordinates to the iron center of ferrous **TCP** in the THF solution and that the pyridine moiety is an axial fifth ligand in ferrous **TCP**−**PY** regardless of a solvent. On exposure to CO gas, ferrous **TCP** in THF and **TCP**−**PY** in toluene are converted to their CO adducts (Figure 2). The reversible CO binding to **TCP** is confirmed by CO/N_2 exchange.

Table 2. Electronic Absorption Data for Iron(II) **TCP**s

complex	solvent	λ_{max}/nm
(**TCP**)Fe^{II}	toluene	417, 445, 538
(**TCP**)Fe^{II}	THF	432, 546
(**TCP**)Fe−CO	THF	422, 538
(**TCP**−**PY**)Fe^{II}	toluene	431, 534
(**TCP**−**PY**)Fe−CO	toluene	428, 541
(**TCP**−**TB**)Fe−CO	THF, −80 °C	373, 456
(**TCP**−**TG**)Fe−CO	THF, −80 °C	364, 452

On the other hand, the ferrous-thiolate-coordinated hemes, **TCP**−**TB** and **TCP**−**TG**, generated by dithionite reduction, form CO adducts which do not exhibit a hyperporphyrin spectrum (**TCP**−**TB**: 422, 538 nm, **TCP**−**TG**: 423, 538 nm in THF). These absorption spectra are identical to reported spectra of six-coordinate ferrous CO adducts bearing a neutral (protonated) thiol ligand.[15] These results suggest that the thiolate group was protonated to yield the thiol during the reduction of the ferric form in a protic media.[16] We selected nonaqueous conditions for the reduction, and decamethylcobaltocene [(Me_5-

(14) Collman, J. P.; Brauman, J. I.; Doxsee, K. M.; Halbert, T. R.; Bunnenberg, E.; Linder, R. E.; La Mar, G. N.; Del Gaudio, J.; Lang, G.; Spartalian, K. *J. Am. Chem. Soc.* **1980**, *102*, 4182.

(15) Collman, J. P.; Groh, S. E. *J. Am. Chem. Soc.* **1982**, *104*, 1391.

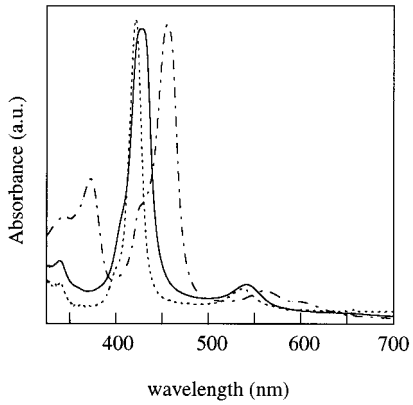

Figure 2. UV−vis spectra of CO adducts: broken line, **TCP** in THF at room temperature; full line, **TCP**−**PY** in toluene at room temperature; dash−dot line, **TCP**−**TB** in THF at −80 °C.

$Cp)_2Co$] was used as a reductant.[17] Its redox potential (−1.47 vs SCE) is low enough to reduce the ferric form of these thiolate complexes. The THF solution of ferric **TCP**−**TB** or **TCP**−**TG** is cooled to −80 °C under CO atmosphere, and then a slight excess of the cobaltocene solution (1.5 molar equiv to the amount of porphyrins) is added. This reaction induces an immediate and drastic change in the UV−vis spectra. A hyperporphyrin spectrum, which is typical for a thiolate-ligated iron(II) porphyrin-CO adduct such as cytochrome P450s, appears with split Soret bands (Figure 2 and Table 2). The Soret band of the ferrous-CO adduct of **TCP**−**TG** is slightly blue-shifted compared with that of **TCP**−**TB**, indicating the decreased electron-donating ability of the thiolate ligand of **TCP**−**TG**.

Vibrational Data of CO Adducts. In Figure 3 are shown the RR spectra of the CO adduct of **TCP** in THF. The CO isotopic substitutions clearly reveal two sensitive bands at 506 and 489 cm^{-1} for **TCP**−$^{12}C^{16}O$ which shift to 503, 488 cm^{-1} upon substitution by $^{13}C^{16}O$, to 500, 485 cm^{-1} by $^{12}C^{18}O$, and to 499, 484 cm^{-1} by $^{13}C^{18}O$. As the total mass of CO gas increases, the 506 cm^{-1} band shifts to lower frequencies with decreased intensity. In contrast, the 489 cm^{-1} band shifts with increased intensity. No additional lines appear to be sensitive to the isotopes of carbon monoxide. Therefore, we assign these two bands as ν(Fe−CO). The reason for the two bands is described below. It is well known that the CO molecule ligated to the ferrous form is readily photodissociable and that the mixture of the CO complex and the CO-free ferrous form is observed during the photoexcitation.[18] However, in this case, the oxidation marker band (ν_4) at 1343 cm^{-1}, indicative of a formation of the CO-free ferrous form, is detected only as a small shoulder in the lower region of the strong 1364 cm^{-1} (ν_4) band. The IR spectrum of **TCP**−$^{12}C^{16}O$ exhibits a strong band at 1990 cm^{-1} (Figure 4). By replacing $^{12}C^{16}O$ with $^{13}C^{16}O$, this band shifts to 1946 cm^{-1}. The observed isotopic shift (44 cm^{-1}) is in good agreement with the value (45 cm^{-1}) calculated from the harmonic oscillator approximation of the C−O stretching vibration. It is therefore assigned as ν(C−O).

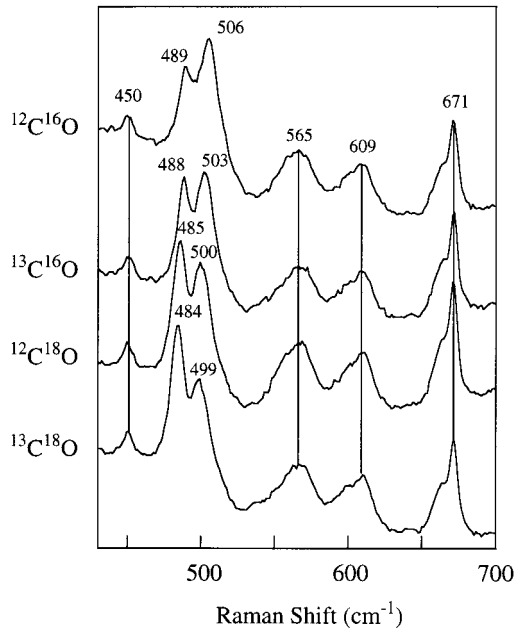

Figure 3. RR spectra of CO adduct of **TCP**. THF, room temperature, 413.1 nm excitation, 5 mW.

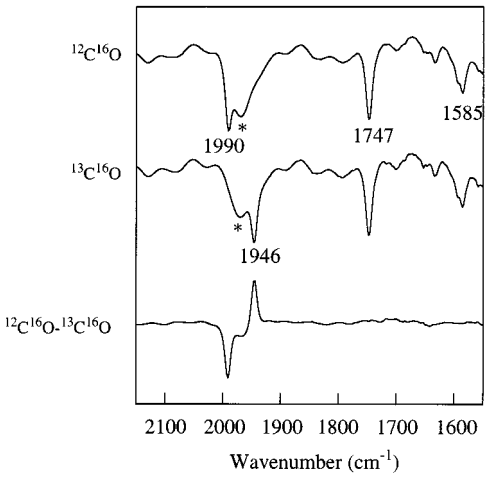

Figure 4. IR spectra of CO adduct of **TCP** in THF. The asterisks denote the solvent peaks.

Low frequency (350−650 cm^{-1}) RR spectra of **TCP**−**PY**−CO in toluene are shown in Figure 5. For **TCP**−**PY**−CO, the ν(Fe−CO) frequency appears at 465 cm^{-1} for $^{12}C^{16}O$ and shifts to 460 cm^{-1} upon substitution by $^{13}C^{16}O$, to 456 cm^{-1} by $^{12}C^{18}O$, and to 452 cm^{-1} by $^{13}C^{18}O$. No other CO sensitive vibrations, corresponding to δ(Fe−C−O), are detectable in this solvent. However, a CO sensitive weak band, which we tentatively assign as the δ(Fe−C−O) mode, was observed in THF around 560 cm^{-1} for $^{12}C^{16}O$ and shifts to 550 cm^{-1} upon substitution by $^{13}C^{16}O$.[19] In this CO adduct, the ν_4 band of the CO-free ferrous form is not observed. The IR spectrum of **TCP**−**PY**−$^{12}C^{16}O$ exhibits a ν(C−O) band at 2008 cm^{-1}.

RR spectra of thiolate-coordinated heme complexes were measured at −80 °C with 441.6- and 457.8-nm laser excitation. Figure 6 displays the RR spectra in the 350−600 cm^{-1} region

(16) To deprotonate the thiol, the addition of various bases to the CO adducts was attempted at −80 °C. When a THF solution of *t*-BuOK was added to the thiol forms, the spectra gradually changed to give split Soret bands around 360 and 450 nm, indicating the formation of the CO adducts with the thiolate axial ligand.

(17) (a) Robbins, J. L.; Edelstein, N.; Spencer, B.; Smart, J. C. *J. Am. Chem. Soc.* **1982**, *104*, 1882. (b) Connelly, N. G.; Geiger, W. E. *Chem. Rev.* **1996**, *96*, 877.

(18) Champion, P. M.; Gunsalus, I. C.; Wagner, G. C. *J. Am. Chem. Soc.* **1978**, *100*, 3743.

(19) However, the unambiguous assignment is difficult because this band was overlapped with another porphyrin band.

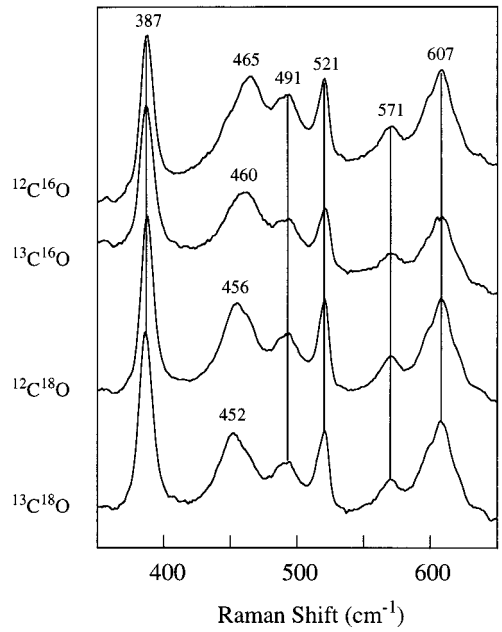

Figure 5. RR spectra of CO adduct of **TCP−PY**. Toluene, room temperature, 413.1 nm excitation, 15 mW.

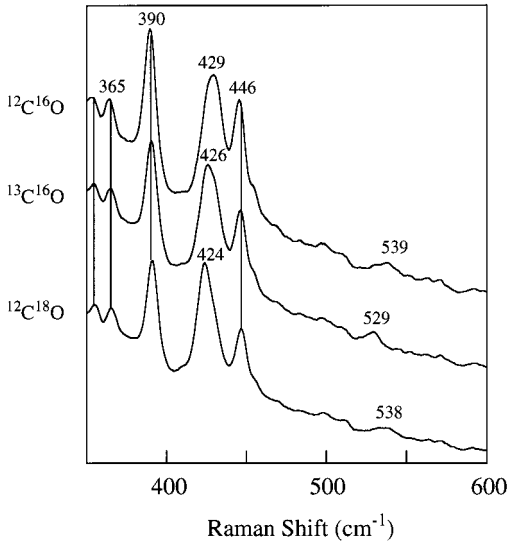

Figure 6. RR spectra of CO adduct of **TCP-TB**. THF, −80 °C, 457.9 nm excitatin, 20 mW.

of $^{12}C^{16}O$, $^{13}C^{16}O$, and $^{12}C^{18}O$ adducts of **TCP−TB** obtained with excitation at 457.9 nm. The strong band at 429 cm^{-1} predictably shifts to lower frequencies with an increase of the total mass of CO. Therefore, this band is assigned to the ν-(Fe−CO) mode. Another weak CO sensitive band is located at 539 cm^{-1}, which shifts to 529 cm^{-1} with $^{13}C^{16}O$ and to 538 cm^{-1} with $^{12}C^{18}O$. There is an alternating (so-called zigzag) shift pattern when comparing the isotopomer spectra in the order given in Figure 6 ($^{12}C^{16}O$, $^{13}C^{16}O$, $^{12}C^{18}O$); large shifts are observed only when the carbon atom is substituted. Such behavior is often seen for the bending of the MXY unit, where the X atom is bonded to a heavy metal center.[20] Therefore, we assign it as the δ(Fe−C−O) mode.

(20) Kincaid, J. R. In *Resonance Raman spectra of Heme Proteins and Model Compounds, Vol 7*: *The porphyrin Handbook*; Kadish, K. M., Smith, K. M., Guilard, R., Eds.; Academic Press: New York, 2000; p 225.

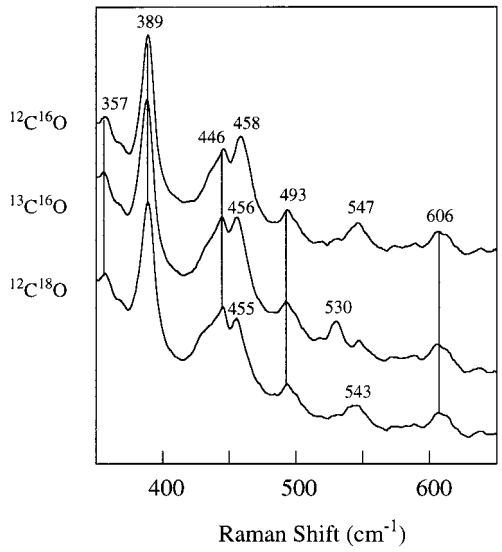

Figure 7. RR spectra of CO adduct of **TCP-TG**. THF, −80 °C, 441.6 nm excitation, 20 mW.

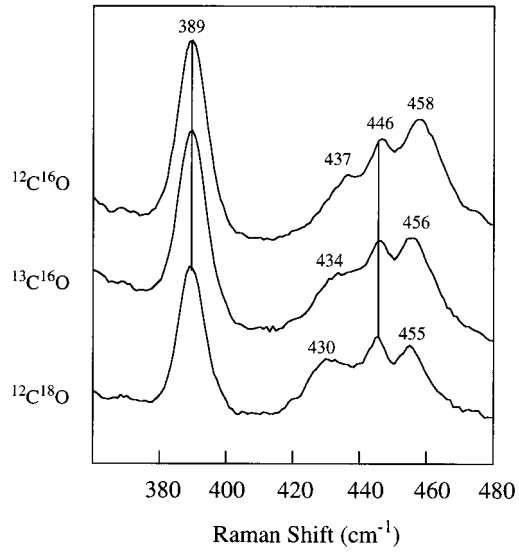

Figure 8. Selected region of RR spectra of CO adduct of **TCP−TG**. THF, −80 °C, 457.9 nm excitation, 15 mW.

On the other hand, the RR spectra of the other thiolate-ligated heme, **TCP−TG**, show complicated isotope shifts upon CO substitution. Figure 7 displays the RR spectra in the 350−600 cm^{-1} region of $^{12}C^{16}O$, $^{13}C^{16}O$, and $^{12}C^{18}O$ adducts of **TCP−TG** excited at 441.6 nm. The CO sensitive band is located at 547 cm^{-1} and shifts to 530 cm^{-1} upon substitution by $^{13}C^{16}O$ and shifts to 543 cm^{-1} upon substitution by $^{12}C^{18}O$. Since it exhibits the same zigzag pattern as observed for **TCP−TB**, this band is also assigned as the δ(Fe−C−O) mode. The observed band at 458 cm^{-1} slightly shifts to lower frequencies by the CO isotopic substitutions. In consideration of experimental accuracy ($\pm$1 cm^{-1}), these shifts are significant values. In addition, with the increase of CO mass, a weak signal is observed in the region slightly lower than the 446 cm^{-1} band. To assign ν(Fe−CO) mode definitely, 457.8 nm excited RR spectra of **TCP-TG**−CO were also measured. Figure 8 shows selected region (360−480 cm^{-1}) of RR spectra of **TCP−TG**−CO adducts. While the shifts of the 458 cm^{-1} band are absolutely identical to those of 441.6 nm excitation, another

Table 3. Raman Frequencies (cm^{-1}) of Porphyrin Skeletal Bands in Iron **TCP**s

complex	solvent	ν_4		ν_2
(**TCP**)Fe^{II}	toluene	1347	1434, 1450, 1481, 1497	1544
(**TCP**)Fe^{II}	THF	1343	1428, 1449, 1486	1541
(**TCP**)Fe−CO	THF	1364	1453, 1487, 1496	1566
(**TCP**−**PY**)Fe^{II}	toluene	1357	1431, 1482	1545, 1563
(**TCP**−**PY**)Fe^{II}	THF	1356	1450, 1490	1563
(**TCP**−**PY**)Fe−CO	toluene	1363	1450, 1491	1565
(**TCP**−**PY**)Fe−CO	THF	1363	1448, 1493	1561
(**TCP**−**TB**)Fe−CO	THF	1362	1449, 1495	1563
(**TCP**−**TG**)Fe−CO	THF	1363	1449, 1495	1567

CO sensitive band is clearly observed at 437 cm^{-1}. Therefore, we also assign these two bands as ν(Fe−CO). The isotopic shift patterns of these two ν(Fe−CO) bands are similar to those of **TCP**−CO in THF.

Table 3 summarizes the Raman frequencies of the porphyrin skeleton bands in iron "twin coronet" porphyrins. These Raman bands in the high-frequency region are known to be sensitive to variations in the oxidation or spin state of the iron atom.[8a] The values of the ν_4 band are classified into three groups: (**TCP**)Fe^{II}: 1343, 1347 cm^{-1}, (**TCP**−**PY**)Fe^{II}: 1356−1357 cm^{-1}, and their CO adducts: 1362−1364 cm^{-1}. The ν_4 band, which can be clearly identified without interference from other modes, is sensitive to the electron population in the π^* antibonding orbitals of the porphyrin ring. When the π^* orbital increases in population, the frequency of ν_4 decreases. Hence, the classification of the ν_4 band values is rationalized by the π-acceptor characteristics of the ligands. Pyridine, which has π-acceptor ability,[21] decreases the electron density of the π^* orbital through Fe dπ orbital, leading to the increase of the ν_4 bands. The CO molecule also functions as a π-acceptor ligand and therefore increases the bands. The next intense bands, which are sensitive to the spin state, are observed around 1541−1567 cm^{-1} and are assigned as the ν_2 mode. We observed that ν_2 bands of high-spin hemes are lower in frequency and much weaker in intensity than ν_2 of low-spin hemes. The lower value of ~1540 cm^{-1} for the five-coordinate Fe^{II} complex is particularly notable. This band is well resolved from the ν_2 band of the six-coordinate Fe^{II} complex and can be used as a specific indicator for five-coordinate species in studies of binding equilibrium.

The two CO isotope sensitive bands assigned to ν(Fe−CO) mode are observed in the CO adducts of **TCP** and **TCP**−**TG**. Some possibilities include: (i) a Fermi doublet, (ii) a mixture of mono and bis CO adducts, (iii) a mixture of five- and six-coordinate adducts; dissociation of the axial ligand trans to CO by the laser beam, or (iv) a vibrational coupling effect of ν(Fe−CO) mode with other modes. First of all, the photodissociation of these CO adducts is effectively lowered because the ν_4 and the other spin marker bands support the six-coordinate form. Second, the ν(Fe−CO) mode of the bis-CO adducts of heme-5 and OEP formed at high CO pressure in benzene have been reported at 498−500 cm^{-1}.[22] However, it is unlikely that **TCP** and **TCP**−**TG** form bis-CO adducts in THF solution. The ν(Fe−CO) frequency of **TCP**−**TG**−CO is extremely low, and therefore, the formation of the bis-CO adduct is ruled out. Finally, each ν(Fe−CO) band shifts by CO isotope substitution in a unique fashion. The higher frequency bands shift to lower frequencies with decreasing intensity. On the other hand, the lower frequency bands shift to lower frequencies with increasing intensity. Each of the shift values is smaller than the value calculated from the harmonic oscillator approximation of Fe−CO stretching vibration. However, the totals of shifts were close to the calculated shifts. Considering these experimental results, the first three possibilities discussed above can be excluded and the vibrational coupling effect of ν(Fe−CO) mode with other modes seems to be the most likely reason for these observations.[23]

RR spectra of heme proteins and models frequently exhibit FeCO bending modes with variable intensity.[20] In this experiment, the FeCO bending mode enhancement is observed for **TCP**−**PY**−CO (in THF), as well as for **TCP-TB**−CO and **TCP-TG**−CO adducts, but is not detected in **TCP**−CO and **TCP**−**PY**−CO adducts in nonpolar solvent. From comprehensive studies of CO adducts to date, it is known that off-axis binding and the electronic influences in the vicinity of the bound CO such as hydrogen bonding and polar interaction are involved in enhancement of the FeCO bending mode.[10,24] Therefore, the lack of δ(Fe−C−O) intensity in a high-symmetry heme−CO adduct (for example, **TCP**−CO) is reasonable. Despite the symmetry reduction, the FeCO bending mode is not enhanced for **TCP**−**PY**−CO in nonpolar solvent. Thus, the activation of the FeCO bending mode depends on the reduction of the molecular symmetry and electronic influences on bound CO in **TCP**s.

We demonstrate the effect of the fifth axial ligand upon the strength of the Fe−C bond by systematic alteration of the ligand of the **TCP**s. Because of the absence of Fe−CO distortion, the Fe−C stretching frequency can be considered as indicative of bond strength; the Fe−C bond strength decreases in the order THF > py > **TG** (thioglycolate) > **TB** (thiobenzyloxy). On the basis of thorough investigations of CO adducts to date,[25−27] these results can be construed as follows: THF, being a weak σ-donor and not a π-acceptor, does not compete significantly with CO ligand for Fe d_{z^2} orbital and does not interfere with the Fe−CO back-bonding; this leads to an increase in the Fe−CO frequency. In contrast, pyridine, being a moderate σ-donor and having increased π-acceptor ability,[21] decreases the iron back-donation toward CO. As a consequence, the Fe−C bond is weakened. Thiolate is a stronger donor ligand than nitrogenous bases, and this increased electron donor capability explains the expected increase in back-donation to the CO π^* orbitals from the more electron-rich Fe. π-Bonding arguments alone would

(21) Spiro, T. G.; Burke, J. M. *J. Am. Chem. Soc.* **1976**, *98*, 5482.
(22) Kerr, E. A. Ph.D. Dissertation, Georgia Institute of Technology, Atlanta, GA, 1984.
(23) Vibrational couplings were also observed in the dioxygen adduct of cobalt porphyrin. (a) Odo, J.; Imai, H.; Kyuno, E.; Nakamoto, K. *J. Am. Chem. Soc.* **1988**, *110*, 742. (b) Proniewicz, L. M.; Kincaid, J. R. *Coord. Chem. Rev.* **1997**, *161*, 881.
(24) Yu, N.-T.; Kerr, E. A.; Ward, B.; Chang, C. K. *Biochemistry* **1983**, *22*, 4534.
(25) Kerr, E. A.; Mackin, H. C.; Yu, N.-T. *Biochemistry* **1983**, *22*, 4373.
(26) Chottard, G.; Schapracher, M.; Ricard, L.; Weiss, R. *Inorg. Chem.* **1984**, *23*, 4557.
(27) Ray, G. B.; Li, X.-Y.; Ibers, J. A.; Sessler, J. L.; Spiro, T. G. *J. Am. Chem. Soc.* **1994**, *116*, 162.
(28) Kerr, E. A.; Yu, N.-T.; Bartnicki, D. E.; Mizukami, H. *J. Biol. Chem.* **1985**, *260*, 8360.
(29) Ramsden, J.; Spiro, T. G. *Biochemistry*, **1989**, *28*, 3125.
(30) Fuchsman, W. H.; Appleby, C. A. *Biochemistry* **1979**, *18*, 1309.
(31) Uno, T.; Nishimura, Y.; Makino, R.; Iizuka, T.; Ishimura, Y.; Tsuboi, M. *J. Biol. Chem.* **1985**, *260*, 2023.
(32) O'Keefe, D. H.; Ebel, R. E.; Peterson, J. A.; Maxwell, J. C.; Caughey, W. S. *Biochemistry* **1978**, *17*, 5845.
(33) Schappacher, M.; Ricard, L.; Weiss, R.; Montiel-Monotoya, R.; Gonser, U.; Bill, E.; Trautwein, A. *Inorg. Chim. Acta* **1983**, *78*, L9.

Table 4. Vibrational Frequencies and Isotope Shifts (cm^{-1}) of **TCP**s−CO Complexes and Reported Iron Porphyrins

complex/solvent	ν_{FeCO}	$\Delta^{13}C^a$	$\Delta^{18}O^a$	ν_{CO}	$\Delta^{13}C^a$	δ_{FeCO}	$\Delta^{13}C^a$	$\Delta^{18}O^a$	ref
FeTPivP(THF)/THF	526	5	10	1957					25, 22
TCP(THF)/THF	506	3	6	1990	44				this work
	489	1	4						
Sperm whale Mb, pH 7.0	507	3		1947		575	16		29, 30
FeTPP(py)/benzene	484	4	9	1976	43				28
TCP−**PY**/toluene	465	5	9	2008	44				this work
cyt P-450_{cam} + camphor pH 7.4	481	3	8	1940	43	558	14	3	31, 32
cyt P-450_{cam} − camphor pH 7.4	464		9	1963	45				31, 32
FeTPivP($C_6HF_4S^-$)/Ph−Cl	479	5		1956					26, 33
TCP−**TG**/THF	458	2	3			547	17	4	this work
	437	3	7						
TCP−**TB**/THF	429	3	5			539	10	1	this work

[a] $\Delta^{13}C$ and $\Delta^{18}O$ are isotope shifts for $^{13}C^{16}O$ and for $^{12}C^{18}O$.

suggest a stronger Fe−C bond associated with the increased back-bonding. However, the σ-bonding interactions of the thiolate and CO ligands compete for the same Fe d_{z^2} orbital so that stronger σ-bonding from thiolate may weaken the Fe−C σ-bond, and this effect apparently predominates. The higher frequency of ν(Fe−CO) of **TCP**−**TG** compared to that of **TCP**−**TB** is ascribed to the coordination of the less σ-donating thiolate ligand relative to that of **TCP**−**TB**. The presence of the carbonyl group at the α position of the thiolate in **TCP**−**TG** could weaken the σ-donation of the thiolate ligand. Electrochemical studies support this argument (Fe^{3+}/Fe^{2+} redox potential: **TCP**−**TB**, −1.35 V; **TCP**−**TG**, −1.12 V; vs Fc/Fc^+ in CH_3CN).[7c]

The vibrational frequencies and the isotope shifts in the previously reported and present CO adducts are summarized in Table 4. The comparison of the reported ν(Fe−CO) frequencies of hemoproteins and their model systems clearly shows that each value of the **TCP**s is significantly lower (ca. 20 cm^{-1}) than the previous adducts having the same kind of axial ligand. Moreover, the ν(C−O) frequencies in IR are abnormally high. Several researchers have examined the strong negative correlation between ν(Fe−CO) and ν(C−O).[8a,10−12] The negative correlation is attributable to Fe $d_\pi \rightarrow$ CO π^* back-donation; as this decreases, the Fe−C bond order decreases and the C−O bond order increases. When ν(Fe−CO) is plotted against ν(C−O) for a variety of CO adducts of heme proteins having proximal histidine ligands, or for model heme−CO adducts having imidazole or pyridine ligands trans to the CO, most of the points fall on a single straight line. Large deviations from this line are observed for complexes with trans ligands that are significantly stronger (imidazolate or thiolate anion) or weaker donors (THF or noncoordinating solvent) than imidazole. When the heme−CO adducts with strong or weak donors are plotted, new two linear correlation, lying below or above the imidazole correlation, are observed. The **TCP**−**PY**−CO point is on the imidazole line, but it is located at far right bottom (Figure 9). The **TCP**−CO point is also located at far right bottom of the weak donor line. There are no previous examples of such low ν(Fe−CO) and high ν(C−O) values. Li and Spiro[10] have suggested that proton donors adjacent to the O atom of the bound ligand enhance the degree of back-bonding, increasing the order of the Fe−C bond and decreasing the order of the C−O bond because of the formation of $Fe^{\delta(+)}{=}C{=}O^{\delta(-)}$ resonance structure (**I**) (Scheme 2). The presence of negative electrostatic potentials next to the oxygen atom is expected to have the opposite effect, decreasing the order of the Fe−C bond and forming

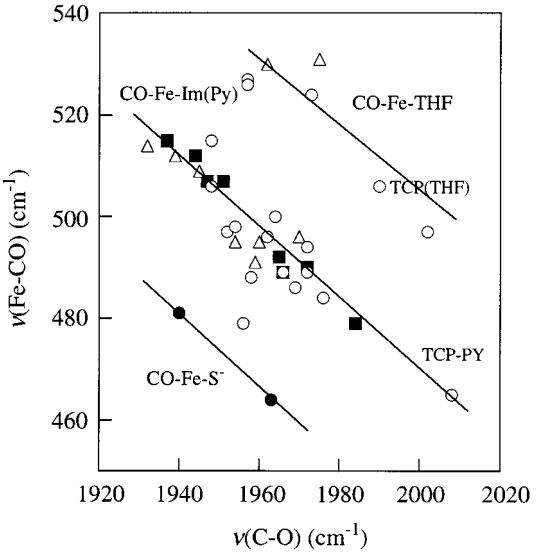

Figure 9. Plot of observed ν(Fe−CO) vs ν(C−O) frequencies in Fe^{II}−CO heme adducts of tetra-aryl porphyrins (open circles), C_β-alkyl porphyrin (open triangles), globins (solid squares), cytochrome P450s (solid circles). The lines are defined by both models and proteins. Data are quoted from ref 26.

$Fe^{\delta(-)}{-}C{\equiv}O^{\delta(+)}$ resonance structure (**III**). Recent publications[27,34] have provided support for the theory that polarity plays the key role in governing the stretching frequency of bound carbon monoxide. The His(E7)Val, Val(E11)Thr double mutant of pig Mb [H64V−V68T] gives rise to an abnormally high ν-(C−O) frequency, 1984 cm^{-1}, and to an abnormally low ν-(Fe−CO) frequency, 479 cm^{-1}.[34b,c,35] These vibrational frequencies in FeCO unit were interpreted in terms of an interaction between the bound ligand and the partial negative charge on the threonine hydroxyl group.[34b,c] Therefore, our present results can be explained by a similar strong negative polar effect. In

(34) (a) Quillin, M. L.; Arduini, R. M.; Olson, J. S.; Phillips, G. N., Jr. *J. Mol. Biol.* **1993**, *234*, 140. (b) Cameron, A. D.; Smerdon, S. J.; Wilkinson, A. J.; Habash, J.; Helliwell, J. R.; Li, T.; Olson, J. S. *Biochemistry* **1993**, *32*, 13061. (c) Li, T.; Quillin, M. L.; Phillips, G. N., Jr.; Olson, J. S. *Biochemistry* **1994**, *33*, 1433. (d) Balasubramanian, S.; Lambright, D. G.; Boxer, S. G. *Proc. Natl. Acad. Sci. U.S.A.* **1993**, *90*, 4718.
(35) Biram, D.; Garratt, C. J.; Hester, R. E. In *Spectroscopic of Biological Molecules*; Hester, R. E., Girling, R. B., Eds.; Royal Society of Chemistry: Cambridge, U.K., 1991; p 433.
(36) Moon, R. B.; Richards, J. H. *Biochemistry* **1974**, *13*, 3437.
(37) Satterlee, J. D.; Teintze, M.; Richards, J. H. *Biochemistry* **1978**, *17*, 1456.
(38) Choc, M. G.; Caughey, W. S. *J. Biol. Chem.* **1981**, *256*, 1831.
(39) Perkins, T.; Satterlee, J. D.; Richards, J. H. *J. Am. Chem. Soc.* **1983**, *105*, 1350.
(40) McMahon, M. T.; deDios, A. C.; Godbout, N.; Saltzmann, R.; Laws, D. D.; Le, H.; Halvin, R. H.; Oldfield, E. *J. Am. Chem. Soc.* **1998**, *120*, 4784.

Scheme 2

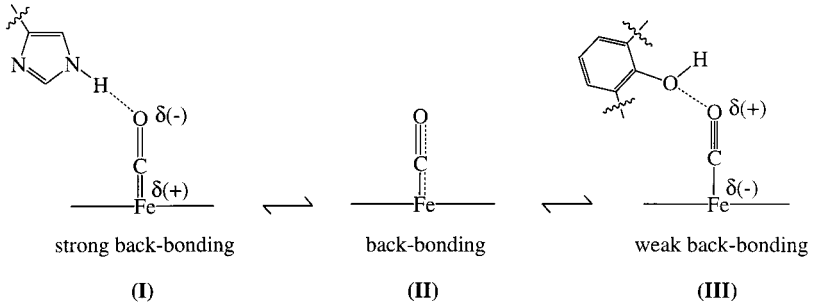

the distal site of **TCP**s, two naphtholic hydroxyl groups are fixed toward the center above the heme. When the CO molecule binds to the heme iron, the lone pairs of the hydroxyl groups may be forced to point toward the bound CO, with a small degree of freedom. This interaction consequently provides a source of negative polarity, and the low ν(Fe−CO) and the high ν(C−O) frequencies are induced. We further investigated the effect of deuterium substitution of the inside hydroxyl protons. After reduction with D_2O solution of dithionite, however, the CO adduct of **TCP**−**PY** showed no meaningful H/D shifts in ν(C−O) and δ(^{13}C) (vide infra) of bound CO. These experimental results indicate the absence of hydrogen-bonding interaction between the hydroxyl groups and bound CO.

^{1}H and ^{13}C NMR of the CO Adducts. ^{1}H NMR spectra of **TCP**−CO and **TCP**−**PY**−CO show signals in the "normal" region of 0−10 ppm, confirming that these adducts are low-spin, diamagnetic species ($S = 0$). However, these spectra are different from those of the corresponding free bases, **5** and **6**. For example, the chemical shifts of the pyridine moiety of **TCP**−**PY**−CO are more strongly shifted upfield (Table 1) by the shielding effect from the porphyrin ring current. The largest shielding effect was observed for the py−H^6 protons (−7.04 ppm, compared with that of methyl nicotinate). This observation clearly indicates coordination of the appended pyridine moiety to the iron center.

When the ^{13}C NMR spectra of **TCP**−^{13}CO and **TCP**−**PY**−^{13}CO are measured at ambient temperature, a single strongly shielded ^{13}C isotopic resonance is observed at 202.6 and 202.3 ppm for **TCP**−CO and **TCP**−**PY**−CO, respectively (Figure 10). ^{13}C shielding of many carbonmonoxy hemoproteins and models vary widely (Table 5) and several researchers have noted a negative correlation between δ(^{13}C) versus ν(C−O) (Figure 11).[9a,d] The δ(^{13}C) parameter also reflects the interaction which is primarily the modulation of π back-bonding via distal pocket polar interactions. A positive potential near CO, as would be the case of the NH dipoles of the amide links, will favor resonance (**I**) (Scheme 2) (decrease in the C−O π-bond order and an increase in the Fe−C π-bond order). If there is a significant increase in π-bonding between the metal and the carbonyl ligand, the carbonyl carbon atom could be deshielded. Negative polar interactions reverse the above effect and favor the other resonance structure (**III**). With the very high ν(C−O) and the highly shielded δ(^{13}C), the points of **TCP**−CO and **TCP**−**PY**−CO are also plotted on the line in the lower right region of the graph, indicating a weaker back-donation. The very significant shielding of the ^{13}C resonances is thought to result from the negative polar effect in the distal site. Hence, the present ^{13}C NMR results also support the presence of the strong negative polar effect in binding site of **TCP**s, as already

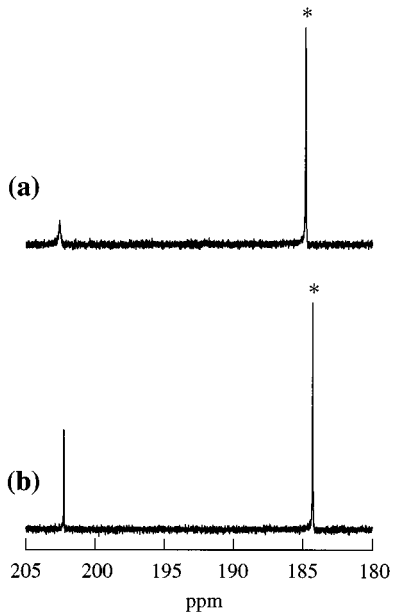

Figure 10. ^{13}C NMR spectra of the ^{13}CO complexes: (a) **TCP** in THF-d_8; (b) **TCP**−**PY** in toluene-d_8. The asterisks denote the signals of dissolved carbon monoxide.

Table 5. ^{13}C Chemical Shifts and ν(C−O) of the CO Adducts of Hemoproteins and Model Complexes

complex	δ(^{13}C)/ppm	ν(CO)/cm^{-1}	ref
rabbit Hb, α chain	208.0	1928	36, 37
sperm whale Mb, pH 7	207.9	1944	39
human Hb, α chain	206.4	1951	36, 38
Fe(TPP)(1-MeIm)	205.0	1969	9d, 40
Fe(TpivP)(1-MeIm)	204.7	1969	9d, 3a
Fe(C_2−Cap)(1-MeIm)	202.1	2002	9d, 41
TCP(THF)	202.6	1990	this work
TCP−**PY**	202.3	2008	this work

shown by RR and IR spectroscopies. The oxygen atom lone pairs of the naphtholic hydroxyl groups are expected to prevent the back-donation from the Fe^{II} d_π to the CO π* orbital. A similar effect has been reported for Fe(C_{2-}Cap)(1-MeIm) complex, which has a benzene cap attached by ester linkages. The high shielding of the ^{13}C resonance ($\delta = 202.1$ ppm) was ascribed to the negative polar effect of the lone pairs of the ester oxygen atoms and the π electron cloud of the benzene ring.[41]

CO Binding Affinity. The CO binding affinity ($P_{1/2}$CO) for **TCP**−**PY** was measured directly by the flow technique.[42] The isosbestic points were maintained during titration. Table 6

(41) Hashimoto, T.; Dyer, R. L.; Crossley, M. J.; Baldwin, J. E.; Basolo, F. *J. Am. Chem. Soc.* **1982**, *104*, 2101.

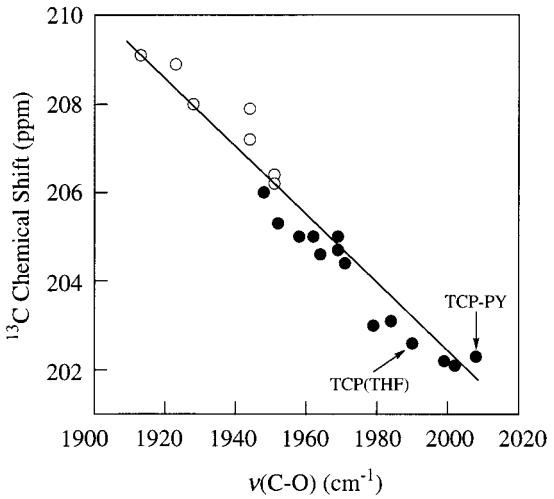

Figure 11. Plot showing the relationship between ^{13}C NMR isotopic chemical shifts and ν(C−O) frequencies for imidazole-coordinated heme models (solid circles) and a variety of proteins (open circles). The line is defined by both models and proteins. Data are quoted from ref 9d.

Table 6. CO Binding Affinity of Iron(II) Porphyrin Complexes

compound	$P_{1/2}$CO (Torr)	conditions	ref
Mb	$1.4-2.5 \times 10^{-2}$	H_2O, 20 °C	44
Hb, R state	$1-4 \times 10^{-3}$	H_2O, 20 °C	45
Hb, T state	$1-2.8 \times 10^{-1}$	H_2O, 20 °C	45
Fe((Piv)$_3$5CImP)	2.2×10^{-5}	toluene, 25 °C	42a
Fe(PFCUPy)	4.9×10^{-5}	toluene, 25 °C	46
Fe−aBHP(C_9Im)(C_{12})	1.7×10^{-5}	toluene, 20 °C	47
Fe−aBHP(C_3·Py·C_3)(C_{12})	9×10^{-5}	toluene, 20 °C	47
Fe(cyclam-capped)-(1,5-DCIm)	$>3.5 \times 10^{3}$	toluene, 25 °C	43
TCP−PY	1.7×10^{-2}	toluene, 25 °C	this work

summarizes CO binding constants for hemoproteins and models. Selected models have intramolecularly linked imidazole or pyridine ligand and no significant steric strain in the distal site, except for Fe(cyclam-capped)(1,5-DCIm) which has an external axial ligand and the extreme steric hindrance in the binding site. The CO affinity of **TCP−PY** is 2−3 order lower than those of other heme models having no steric strain and comparable to that of Mb. It is reasonable to consider that this dramatic decrease of CO affinity is caused by the strong negative polar effect in the distal site, which is revealed by RR, IR, and NMR spectroscopies. Generally, CO binds to a simple heme with a much greater affinity than to Mb and Hb.[2] Collman and co-workers reported thermodynamic and structural studies on numerous iron porphyrin models and demonstrated that steric interactions could dramatically lower the affinity for CO (e.g., Fe(cyclam-capped)(1,5-DCIm)).[43] On the other hand, the present **TCP** complexes are rare examples, in which electrostatic interactions in the distal site play the key role for controlling CO affinity.

Conclusion

In this article, we described the formation and spectroscopic characterization of CO adducts of **TCP**s. By the use of RR spectroscopy, ν(Fe−CO) and δ(Fe−C−O) bands of the CO adducts were determined. The proximal factors affecting the strength of the Fe−C bond were examined by changing the axial ligands. The Fe−C bond strength decreases in the order THF > py > **TG** (thioglycolate) > **TB** (thiobenzyloxy) because of the dependence on both the σ-donor and the π-donor, acceptor characters of the ligands. The ν(Fe−CO) of each of the **TCP** species is significantly lower than the previously reported CO-hemes having the same types of the axial ligand. Moreover, the ν(C−O) bands of **TCP**−CO and **TCP**−**PY**−CO in IR are unusually high. The plots of ν(C−O) and ν(Fe−CO) of **TCP**−CO and **TCP**−**PY**−CO confirmed that the π-back-bonding correlation can be applied to the CO adducts of **TCP**s. We conclude that both the unusually lower ν(Fe−CO) and the unusually higher ν(C−O) frequencies of **TCP**s are caused by the strong negative polar interactions of bound CO with the O atom lone pairs of the distal hydroxyl groups in the cavity. The very significant shielding of the ^{13}C resonances of **TCP**−**PY**−CO also supports this argument. The CO affinity of **TCP**−**PY** was extraordinarily low as models and was close to that of Mb. This property could be caused by the electrostatic effects in the distal site. Such a strong polar effect has been rarely observed in both hemoproteins and models thus far. The present results highlight the importance of the polar interaction in heme-CO chemistry and increase our understanding of the mechanism of CO/O_2 discrimination.

Experimental Section

General Methods. All reagents and solvents were of the commercial reagent grade and were used without further purification except where noted. Purification was made by the standard methods.[48] Preparation and handling of air-sensitive materials were carried out under N_2 in a glovebox (M. Braun 150B−G-II or VAC Dri-Lab-08/85) equipped with a circulating purifier (O_2, H_2O < 1 ppm). Absolute THF and toluene were obtained by redistillation over potassium in a glovebox. Deoxygenation of solvents was achieved by a freeze-and-thaw technique under high vacuum conditions ($<10^{-5}$ Torr).

Instruments. ^{1}H and ^{13}C NMR spectra were recorded on a JEOL JMX-GX400 (400 MHz). High-resolution mass (HR−MS) spectra were recorded by FAB method with nitrobenzyl alcohol as a matrix on a JEOL LMS−HX-110 spectrometer. Electrospray ionization mass (ESI−MS) spectra were obtained on a Perkin-Elmer Sciex API 300 mass spectrometer. UV−vis electronic spectra were recorded on a Shimadzu UV-3100PC spectrophotometer or a HAMAMATSU PMA-11 CCD spectrophotometer with a Otsuka MC-2530 as a light source (D_2/W_2). The temperature was controlled by a NESLAB ULT-95 low-temperature circulator. Infrared spectra were recorded on a BIO RAD FTS-6000 spectrometer. ESR spectra were obtained at liquid-helium temperature on a Bruker ESP 300e spectrometer equipped with an RMC CRYO SYSTEMS CT-470-ESR. Resonance Raman spectra were obtained on an Acton Research SpectraPro-300i spectrograph (operating at a 2400-groove grating) using a Spectra-Physics Beamlok 2060 Kr ion laser (413.1 nm), a KIMMON Electric IK4152R−G He−Cd laser (441.6

(42) (a) Collman, J. P.; Brauman, J. I.; Iverson, B. L.; Sessler, J. L.; Morris, R. M.; Gibson, G. H. *J. Am. Chem. Soc.* **1983**, *105*, 3052. (b) Traylor, T. G.; Tsuchiya, S.; Campbell, D.; Mitchell, M.; Stynes, D.; Koga. N. *J. Am. Chem. Soc.* **1985**, *107*, 604.
(43) (a) Collman, J. P.; Fu, L. *Acc. Chem. Res.* **1999**, *32*, 455. (b) Collman, J. P.; Herrmann, P. C.; Fu, L.; Eberspacher, T. A.; Eubanks, M.; Boitrel, B.; Hayoz, P.; Zhang, X.; Brauman, J. I.; Day, V. W. *J. Am. Chem. Soc.* **1997**, *119*, 3481.
(44) Antonini, E.; Brunori, M. *Hemoglobin and Myoglobin in their Reactions with Ligands*; Elsevier: New York, 1971; p 221.
(45) (a) MacQuarrie, R.; Gibson, Q. H. *J. Biol. Chem.* **1971**, *246*, 5832. (b) Sharma, V. S.; Schmidt, M. R.; Ranney, H. M. *J. Biol. Chem.* **1976**, *251*, 4267.
(46) Collman, J. P.; Brauman, J. I.; Doxsee, K. M.; Sessler, J. L.; Morris, R. M.; Gibson, Q. H. *Inorg. Chem.* **1983**, *22*, 1427.
(47) Momenteau, M.; Loock, B.; Lavalette, D.; Tetreau, C.; Mispelter, J. *Chem. Soc., Chem. Commun.* **1983**, 962.
(48) Perrin, D. D.; Armarego, W. L. F. *Purification of Laboratory Chemicals*, 3rd ed.; Pergamon Press: Oxford, 1988.

nm), or a Spectra-Physics Stabilite 2017 Ar ion laser (457.8 nm), a Kaiser Optical holographic supernotch filter, and a Princeton Instruments (LN-1100PB) liquid-N_2-cooled CCD detector. Spectra were collected on solution samples in spinning cells (2-cm diameter, 1500 rpm) with a laser power of 5−20 mW, 90° scattering geometry, and 5−20 min data accumulation. The temperature was monitored with a thermocouple at the sample point and controlled by the flow rate of cold nitrogen gas, which flowed through liquid N_2 to a cell in a quartz dewar. Peak frequencies were calibrated relative to indene and CCl_4 standards and were accurate to ± 1 cm^{-1}. During each Raman experiment, UV−vis spectra were simultaneously collected on a HAMAMATSU PMA-11 CCD spectrophotometer with Otsuka MC-2530 as a light source (D_2/W_2). The isotope-substituted complexes were prepared with $^{13}C^{16}O$ (Cambridge Isotope Lab, 99 atom % for ^{13}C), $^{12}C^{18}O$ (ICON, 95 atom % for ^{18}O), and $^{13}C^{18}O$ (ICON, 99 atom % for ^{13}C and 95 atom % for ^{18}O). The partial pressure of CO in N_2 was controlled with a KOFLOC gas blender GB-3C in CO affinity experiment.

Synthesis. The synthesis of **1**−**5**, **TCP**−**TB,** and **TCP**−**TG** has already been reported elsewhere.[7]

6. To a CH_2Cl_2 solution (3 mL) of **5** (20 mg, 8.6×10^{-3} mmol), 4-(dimethylamino)pyridine (53 mg, 0.43 mmol), 1-(3-dimethylaminopropyl)-3-ethylcarbodiimide hydrochloride (82 mg, 0.43 mmol) and nicotinic acid (53, 0.43 mmol) were added and stirred at room temperature in the dark. After 2 h, the portion of the solution was taken, was washed with 1*N* HCl and saturated aqueous $NaHCO_3$, and then was extracted with CH_2Cl_2. The formation of **6** was checked by TLC. Before the formation of the undesired compound, in which the two hydroxyl groups were esterified, the reaction mixture was quenched with 1*N* HCl and then was extracted with CH_2Cl_2. The combined organic layer was washed successively with saturated aqueous $NaHCO_3$, brine, and then was dried over Na_2SO_4. After evaporation of the solvent, the crude product was purified by flash column chromatography (silica gel, CH_2Cl_2/EtOH). **6** was obtained as purple solids (12 mg, 4.95×10^{-3} mmol, 57%). ^1H NMR (400 MHz, $CDCl_3$) 8.91 (d, $J = 4.6$ Hz, 1H, pyrrole β-H), 8.86 (d, $J = 4.4$ Hz, 1H, pyrrole β-H), 8.70 (d, $J = 4.4$ Hz, 1H, pyrrole β-H), 8.64 (d, $J = 4.6$ Hz, 1H, pyrrole β-H), 8.62 (d, $J = 4.6$ Hz, 1H, pyrrole β-H), 8.55 (d, $J = 5.1$ Hz, 1H, pyrrole β-H), 8.19 (d, $J = 4.6$ Hz, 1H, pyrrole β-H), 8.14 (d, $J = 4.6$ Hz, 1H, pyrrole β-H), 8.07 (s, 1H), 7.98 (d, $J = 8.3$ Hz, 1H), 7.94 (s, 1H), 7.88 (s, 1H), 7.81 (s, 1H), 7.80 (d, $J = 6.6$ Hz, 1H), 7.75−7.66 (m, 3H), 7.60 (t, $J = 8.5$ Hz, 1H), 7.59 (s, 1H), 7.54−7.48 (m, 5H), 7.44 (d, $J = 8.1$ Hz, 1H), 7.39 (d, $J = 8.3$ Hz, 1H), 7.32−6.95 (m, 18H), 6.85−6.74 (m, 5H), 6.70 (d, $J = 8.5$ Hz, 1H), 6.63−6.53 (m, 4H), 6.47 (d, $J = 8.5$ Hz, 1H), 6.37 (d, $J = 8.5$ Hz, 2H), 6.33 (d, $J = 4.9$ Hz, 1H, py-H^6), 6.06 (d, $J = 7.8$ Hz, 2H), 5.85 (d, $J = 14.4$ Hz, 1H), 5.83 (d, $J = 14.6$ Hz, 1H), 5.61 (s, 1H, py-H^2), 5.33−5.14 (m, 6H), 5.02−4.78 (m, 5H), 4.32 (dd, $J = 7.8$, 4.9 Hz, 1H, py-H^5), 4.24 (d, $J = 13.7$ Hz, 1H, benzyl-CH_2), 4.13 (d, $J = 13.9$ Hz, 1H, benzyl-CH_2), 3.72 (d, $J = 7.8$ Hz, 1H, py-H^4), 2.67 (d, $J = 13.7$ Hz, 1H, benzyl-CH_2), 2.52 (d, $J = 13.9$ Hz, 1H, benzyl-CH_2), 0.77 (s, 9H, piv-CH_3), 0.73 (s, 9H, Piv-CH_3), 0.24 (s, 9H, piv-CH_3), 0.22 (s, 9H, piv-CH_3), −3.71 (s, 2H, NH); UV−vis (CH_2Cl_2) λ_{max} ($10^{-3}\epsilon$, $M^{-1}\cdot cm^{-1}$) 325 (20.9), 339 (19.9), 423 (222.1), 520 (12.9), 586 (4.7), 640 nm (2.3); IR (neat) 3503, 3325, 3309, 3063, 2958, 2930, 2874, 1747, 1585, 1457, 1367, 1260, 1232, 1111, 1085, 789, 747, 719 cm^{-1}; HR-MS ($C_{158}H_{122}O_{21}N_5$) calcd 2424.8632, found 2424.8621.

TCP−**PY**−**Cl. 6** (12 mg, 4.94×10^{-3} mmol) was dissolved in dry toluene (10 mL) and heated at 50 °C under N_2. $Fe(CO)_5$ (221 μL, 1.65 mmol) and a toluene solution of I_2 (6.8 mg, 56.3×10^{-3} mmol) were added. The mixture was stirred overnight in the dark, was quenched with water, and then was extracted with CH_2Cl_2. After removal of the solvent and drying, the residue was purified by flash column chromatography (silica gel, CH_2Cl_2). The eluent was washed with brine, was dried over NaCl, and was freed from solvent, affording **TCP**−**PY**−Cl (8.6 mg, 3.47×10^{-3} mmol, 70%). UV−vis (CH_2Cl_2) λ_{max} ($10^{-3}\epsilon$, $M^{-1}\cdot cm^{-1}$) 324 (30.8), 403 (90.9), 526 (9.1); IR (neat) 3432, 3056, 2956, 2925, 2854, 1748, 1585, 1456, 1363, 1276, 1259, 1232, 1110, 1082, 997, 787, 747, 719 cm^{-1}; ESR (toluene, 4 K) $g = 5.82$, 2.00; HR−MS ($C_{158}H_{119}O_{21}N_5Fe$) calcd 2477.7747, found 2477.7761; elemental analysis ($C_{158}H_{119}O_{21}N_5FeCl\cdot 8H_2O$) calcd C 71.37, H 5.12, N 2.63; found C 71.05, H 5.59, N 2.58.

TCP−**Cl**. The free-base porphyrin **5** was metalated by a procedure analogous for **TCP**−**PY**−Cl. Yield: 57%. UV−vis (CH_2Cl_2) λ_{max} ($10^{-3}\epsilon$, $M^{-1}\cdot cm^{-1}$) 339 (37), 420 (74.0), 508 (9.5), 582 (3.1); IR (neat) 3455, 3056, 2970, 2933, 2874, 1747, 1586, 1456, 1367, 1275, 1260, 1232, 1110, 1082, 998, 787, 748, 720 cm^{-1}; ESR (toluene, 4 K) $g = 5.96$, 2.01; HR−MS ($C_{152}H_{116}O_{20}N_4Fe$) calcd 2372.7532, found 2372.7520; elemental analysis ($C_{152}H_{116}O_{20}N_4FeCl\cdot 4H_2O$) calcd C 73.56, H 5.04, N 2.26; found C 73.32, H 4.95, N 2.31.

Measurements of CO Affinity. The CO binding affinity (CO pressure at half CO binding for a ferrous heme, $P_{1/2}CO$) was determined by UV−vis spectral change (800−300 nm) under various partial pressures of CO in N_2. The mixed gas was introduced by the flow method.[42] The temperature of the UV−vis cell was regulated at 25.0 ± 0.3 °C with a NESLAB RTE−111 circulator. The concentration of the metalloporphyrin was 10 μM in toluene in a 1-cm cuvette.

Acknowledgment. This research was financially supported by Grant-in-Aids for COE Research (#08CE2005 to Y.N.), for Scientific Research on Priority Areas (#09235225 and 11228207 to Y.N.), and for Encouragement of Young Scientists (#08740500 to F.T.) from the Ministry of Education, Science, and Culture, Japan and by Research Grants to F.T. from Takeda Science Foundation and Otsuka Chemical Co. Ltd. M.M. gratefully acknowledges the Japan Society for the Promotion of Science for the JSPS Research Fellowships for Young Scientists. We thank Dr. Nobuhumi Nakamura (Tokyo University Agr. & Tech.) for his helpful discussions about resonance Raman Spectroscopy and Dr. Koichiro Ishimori (Kyoto University) for his kind suggestions about ^{13}C NMR measurement.

Supporting Information Available: The ^1H NMR spectra of **TCP**−CO and **TCP**−**PY**−CO (PDF). This material is available free of charge via the Internet at http://pubs.acs.org.

JA011963G